

**REVIEW OF EXPERIMENTAL SUB-SYNCHRONOUS VIBRATIONS ON LARGE SIZE TILTING PAD JOURNAL BEARINGS AND COMPARISON WITH ANALYTICAL PREDICTIONS****Mirko Libraschi**

Senior Engineer (Mechanical Engineer)  
GE Oil&Gas Nuovo Pignone  
Florence, Italy

**Oscar Crosato**

Engineer (Mechanical Engineer)  
GE Oil&Gas Nuovo Pignone  
Florence, Italy

**Michael Catanzaro**

Engineer (Mechanical Engineer)  
GE Oil&Gas Nuovo Pignone  
Florence, Italy

**Silvia Evangelisti**

Lead Engineer (Test Project Engineer)  
GE Oil&Gas, Nuovo Pignone  
Florence, Italy



*Mirko Libraschi is a Rotordynamics Senior Engineer for GE Oil&Gas. He works in the Advanced Technology Organization since 2010, specially involved in RCAs and several research activities on bearing. He directly followed Tilting Pad Journal Bearing test campaigns, identification methodology and analytical investigation.*

*Mirko Libraschi received his Mechanical Engineering degree in 2002 at the University of Pisa and before becoming GE employee he works as Member of Engineers register mainly for Torsional Lateral rotordynamic assessment of turbocompressor and turbogenerator train.*



*Silvia Evangelisti is a Lead Test Engineer in GE Oil&Gas Technology Laboratory. She joined GE in 2001, and moved to her current role in 2005, after Engineering Edison Development Program. She has been involved in several projects, from conceptual test design to data analysis, with a special focus on centrifugal compressors validation area. Silvia holds a M.S. degree in Mechanical Engineering from the University of Bologna.*

*Silvia holds a M.S. degree in Mechanical Engineering from the University of Bologna.*

**ABSTRACT**

Tilting pads journal bearing (TPJB) force coefficients are usually evaluated by the Lund approach where pad degrees of freedom are reduced to those of the shaft (8 Synchronous Reduced Coefficients), therefore for each shaft perturbation pads are assumed to simultaneously response. This assumption might not remain valid in the presence of a particular combination of rotor-bearings system and operating condition. In such systems pad inertia leads to a phase delay between the same pad and shaft movement.

Depending on the rotor-bearing system the synchronous reduced assumption may not be accurate to identify the instability threshold speed and an explicit modeling of pad dynamic (degree of freedom) has to be incorporated into the rotordynamic analysis. The synchronous reduced method is still accurate in the determination of threshold speed for current turbomachine technology. For future advanced challenging applications the understanding and definition of the applicability of the reduced method is necessary.

The predicted sub-synchronous instability (negative logarithmic decrement) presented in this paper are calculated by introducing in the finite element model (beam elements) additional nodes (respect to shaft generalized coordinates) at bearing locations to represent the pads degrees of freedom.

The calculations were repeated to predict the instability threshold speed using the classical Lund approach and it has been verified that using this method the instability threshold speed is over predicted with respect to those obtained in the above mentioned analysis. The comparison of the calculations highlights the important difference in the speed threshold



*Michael Catanzaro received the MSc. in Mechanical Engineering from the University of Pisa in 2010. He joined GE Oil&Gas in the 2010 and after the Engineering Edison Development Program he moved to his current role as a Rotordynamic Engineer in the Advanced Technology Organization of GE Oil&Gas. He has been involved into*

*both analytical and experimental rotordynamics research activities on tilting pad journal bearings, squeeze film dampers, balancing and systems identification techniques.*



*Oscar Crosato is a Design Engineer at Nuovo Pignone General Electric Oil & Gas Division, in Florence, Italy. He has been involved in research activities aimed to explore the behavior of the journal bearings at peripheral speed. Dr. Crosato received his Mechanical Engineering degree in 2004 at the University of Rome "La Sapienza",*

*after having obtained his Master of Science Degree in the Gas Turbine "Thermal Power" course at the University of Cranfield (UK) in 2003.*

values given by the two methods for the system considered.

A development activity has been performed to test a configuration of rotor-bearings system of high peripheral speed (> 75 m/s) and large bearing diameter (> 180 mm) verifying the tools prediction capability. The scope of this work is to compare experimental observed sub-synchronous vibration (instability threshold speed) with the predictions in order to consolidate the reliability of the method. To enforce the validation the same test are repeated with different TPJB designs in order to test different bearing configurations in terms of micro-geometry, pad arc length, pivot stiffness etc.

## INTRODUCTION

As part of a research and development program a series of activities oriented to develop turbomachineries equipped with large bearings at high peripheral speed has been performed. During testing unpredicted instability phenomena occurred, due to the lack of predictability a different set of assumptions were investigated with respect to the ones used in the classical tilting pad journal bearing (TPJB) modeling.

According to (Lund, 1964) the rotor motion amplitude can be considered sufficiently small so that the forces acting on the rotor can be linearized around the eccentricity position, thus the force results are proportional to the amplitude and velocity of the vibration. Assuming to know shaft position and speed the pressure profile is found, by 1<sup>st</sup> order perturbation of the solution the equivalent stiffness and damping force coefficients are:

$$K_{ij} = \frac{dF}{du_{ij}} \text{ and } C_{ij} = \frac{dF}{d\dot{u}_{ij}} \quad (\text{Eq. 2})$$

Where  $K_{ij}$  represent stiffness and  $C_{ij}$  damping while  $F$  is the hydrodynamic force obtained integrating the pressure profile on the shaft surface. TPJB dynamic force coefficients are represented for a datum speed by 8 reduced force coefficients (Figure ).

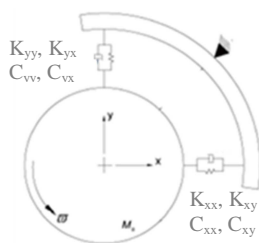


**Figure Synchronous Reduced DOF modeling**

(Shapiro, 1977) included the pad dynamics in the analysis, they considered a five tilting pad bearing, building a 7x7 stiffness matrix where the 2 DOFs of the shaft and the 5 rotations of the pad are taken into account. The improvement of the computational power allowed (Dimond, 2009) to consider the pad rotations and translations in a Thermo Elasto-HydroDynamic (TEHD) finite elements analysis (Figure 1).

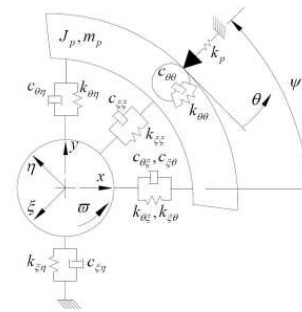


**Figure 1 Full DOF modeling**

Additional pivot flexibility has to be included for the correct evaluation of shaft and pads equilibrium position (Delgado, 2011). Considering both pad rotation and radial motion stiffness and damping matrix dimension becomes 12x12 for a 5 tilting pads journal bearing.

An experimental campaign has been performed to test a configuration of rotor-bearings system with an unusual combination of peripheral speed/system flexibility verifying the method prediction capability.

## TEST CAMPAIGNS SUMMARY

Test campaigns to understand a 200 mm diameter bearing performance and modeling capabilities are presented:

1. In the 1<sup>st</sup> test campaign a bearing of 200 mm diameter was tested (Bearing A). The classical reduced coefficients showed the rotor to be stable up to 12000 rpm but instability threshold appeared at ~7000 rpm. The assumption related to the classical approach to consider bearing rotordynamic 8 coefficients have been questioned. During data post processing the explicit dynamic of the bearing-rotor system has been modeled considering a rigid shaft and two degrees of freedom for each pad (radial and angular). It has been found a resonance condition of the upper pad at the threshold speed, but the high level of damping does not explain the instability experienced, the inaccuracy of the calculation is due to not considering the shaft flexibility and gyroscopic effect. A finite element method has been used to model bearings (considering two degrees of freedom for each pad) and the shaft; the instability threshold speed was well evaluated by the code.

2. In order to validate the methodology a 2<sup>nd</sup> test campaign was performed. Additionally to Bearing A another 200 mm diameter bearing (Bearing B) with different features and characteristics was tested. A different rotor has been used for this second test campaign. The code was able to predict the threshold speed and the frequency of the sub-synchronous vibration for both Bearing A and Bearing B demonstrating the reliability of the method.

## TEST INSTRUMENTATION

### Test rig description

The High Speed Balancing facility in GE O&G Nuovo Pignone has been used for the testing activity. The structure consists of a walk-in tunnel design, the enclosure of the facility protects from the risk of a rotor explosion, all the high speed operations can be performed under vacuum conditions to limit power consumption and temperature due to windage effects. The driver is a three-phase motor, a gearbox is present to allow operations on a wide speed range which is coupled with the testing chamber by a high precision intermediate shaft. In-between the intermediate shaft and the rotor a flexible drive shaft is used in order to decouple as much as possible the intermediate shaft and rotor lateral dynamic, moreover the flexible drive shaft allows minimal misalignment effects.

The pedestals are the same used for high speed balancing operations and they can accommodate a large variety of bearing sizes. The oil flowrate can be controlled by setting the oil pressure at the inlet of each pedestal.



Figure 2 Test Facility

Vibrations can be measured by two different systems:

- Velocimeters in the pedestals (suitable for balancing operations);
- Proximity probes on the pedestals to measure directly rotor relative vibrations.

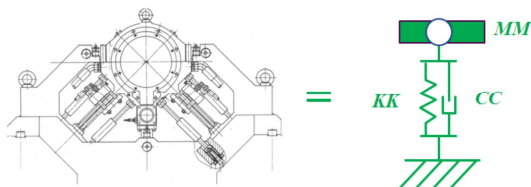


Figure 3 Pedestals scheme

Pedestals resonance frequencies related to the lateral degrees of freedom of the rotor are out of the speed range of interest. A modal identification activity showed that the pedestals dynamic behavior can be described by a single degree of freedom system modeling Static stiffness ( $K = 1740 \text{ N}/\mu\text{m}$ ), modal damping ( $\zeta = 0.01$ ) and modal mass ( $M = 520 \text{ kg}$ ) have been used to include pedestals dynamics in the rotor-bearing-pedestals modeling.

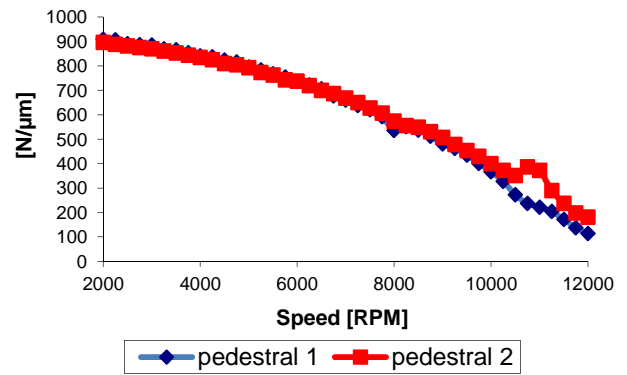


Figure 4 Dynamic Characteristics

### Bearings instrumentation

In all test campaigns, the test instrumentation included:

- Temperature measurements: instrumented pads for temperature measurements have been used to get the thermal characterization of the bearings. Standard PT100 RTDs were installed. The pads were provided with two temperature measurements on the leading and the trailing edges.
- Pad vibrations: Proximity Sensors were installed inside the bearing houses, measuring the two most load/unloaded pads vibrations
- Rotor vibrations: proximity sensors were bounded to the bearing outer shells at the burnishing position. The proximity sensors were calibrated with the actual material target.

Moreover:

- Standard type K thermocouples were installed on the bunker oil piping, at the inlet and outlet of each bearing.
- Lubricant mass flow and pressure measurements were retrieved from the test facility control panel.

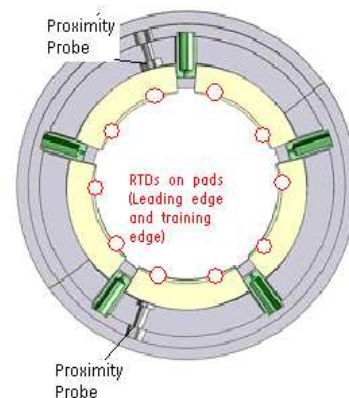


Figure 5 Pads RTD & proximity probes

## TEST CAMPAIGN – JUNE 2011

### Predictions – Classical Lund Approach

The first rotor tested is representative of a “rigid rotor” in order to limit the impact of the shaft flexibility on the bearings performance. The scope of the test was to reach 12000 rpm (test rig limit) and measure steady state temperature on the bearing pads.

Direct lube tilting pad journal bearings with standard clearance were purchased to test the above mentioned rotor.

Below are the most important parameters:

- Bearing span: 2.294 mm
- Total mass: 1783 Kg
- Bearing diameter: 200 mm
- Bearing axial length: 80 mm
- Type of load: Load on pad
- Lubrication: direct
- Test run under vacuum

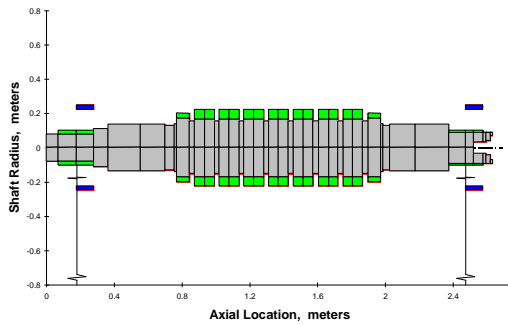


Figure 6 Rotor model

Using the Lund synchronous reduced TPJB force coefficients the predicted logarithmic decrement (log. dec.) at 7000 rpm of the first mode is  $\approx 0.45$  (Figure 7).

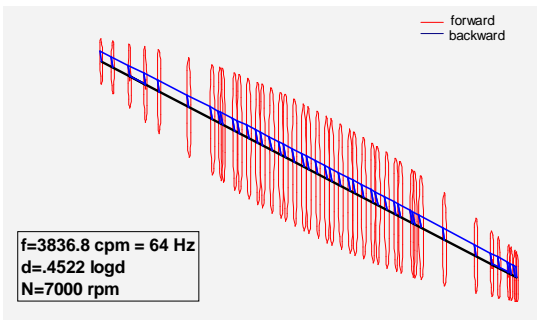


Figure 7 First mode at 7000 rpm

Moreover non-synchronous reduced TPJB force coefficients are used and the predicted logarithmic decrement (Log.Dec.) at 7000 rpm of the first mode remained invariant  $\approx 0.45$ .

### Experimental results

During the test it was observed an unexpected high sub-synchronous vibration (52 Hz  $\approx 200 \mu\text{m}$ ), the threshold speed is around 7000 rpm (Figure 8).

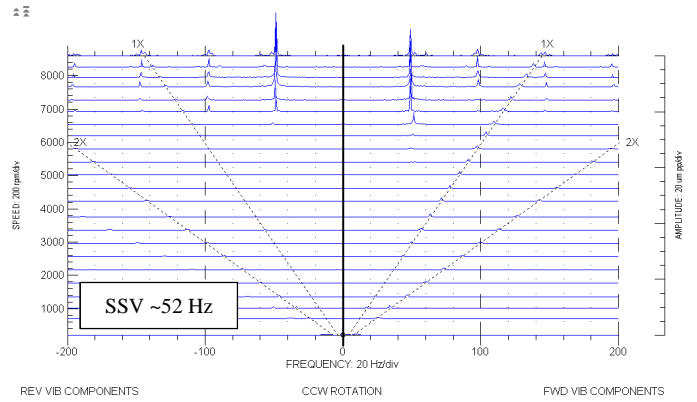


Figure 8 Cascade plot - Threshold speed ~7000 rpm

Based on the experimental result it was possible to conclude that both frequency and logarithmic decrement were over predicted.

### Postprocessing - Full DOFs approach

Due to the lack of predictability on the instability threshold speed and because during the test it was observed that the top pad starts to vibrate at a sub-synchronous frequency before the shaft (Figure 9 Error! Reference source not found.), it was decided to model the journal bearings without assuming a synchronous reduced dynamic. Considering a bearings-rigid shaft system, an eigenvalues calculation was performed in order to evaluate the complex frequency.

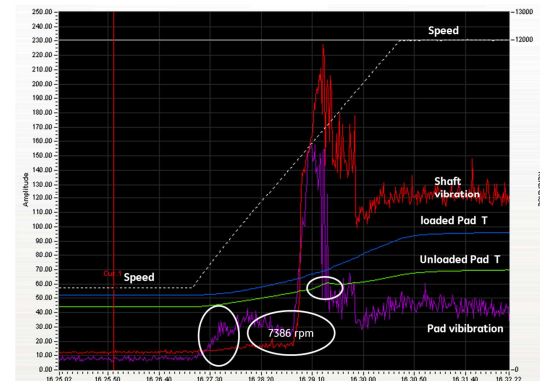


Figure 9 Trend data

Below is reported in a compact matrix representation a second order differential equation system describing the equilibrium of the rigid shaft-bearing system:

$$\begin{bmatrix} M_s & 0 & 0 \\ 0 & J_p & 0 \\ 0 & 0 & M_p \end{bmatrix} \begin{Bmatrix} \ddot{u}_s \\ \ddot{\theta}_p \\ \ddot{\xi}_s \end{Bmatrix} + \begin{bmatrix} C_{uu} & C_{u\theta} & C_{u\xi} \\ C_{\theta u} & C_{\theta\theta} & C_{\theta\xi} \\ C_{\xi u} & C_{\xi\theta} & C_{\xi\xi} \end{bmatrix} \begin{Bmatrix} \dot{u}_s \\ \dot{\theta}_p \\ \dot{\xi}_s \end{Bmatrix} + \begin{bmatrix} K_{uu} & K_{u\theta} & K_{u\xi} \\ K_{\theta u} & K_{\theta\theta} & K_{\theta\xi} \\ K_{\xi u} & K_{\xi\theta} & K_{\xi\xi} + K_p \end{bmatrix} \begin{Bmatrix} u_s \\ \theta_p \\ \xi_s \end{Bmatrix} = \begin{Bmatrix} f \\ 0 \\ 0 \end{Bmatrix}$$

$$[M] \ddot{\vec{q}} + [C] \dot{\vec{q}} + [K] \vec{q} = \vec{F} \quad (\text{Eq. 2})$$

Where  $\vec{u}_s$  represent the coordinate related to the shaft

motion (horizontal  $x$  and vertical  $y$ ), while  $\vec{\theta}_p$  and  $\vec{\xi}_p$  respectively represent pads rotational and radial coordinates. In this representation it is assumed a rigid rotor without considering gyroscopic effects:  $M_s$  represents shaft mass,  $J_p$  and  $M_p$  respectively pad moment of inertia and mass.

The second order differential equations system can be represented in the state space by a first order equations system. The eigenvalues (complex conjugates) of the system characteristics matrix  $A$  represent the eigenvalues of the bearings-rigid shaft.

$$\begin{cases} \dot{\vec{z}} = [A] \vec{z} + [B] \vec{u} \\ \vec{y} = [C] \vec{z} \end{cases} \quad (\text{Eq. 3})$$

$$[A] = \begin{bmatrix} 0 & [I] \\ [M]^{-1}[K] & [M]^{-1}[C] \end{bmatrix} \quad (\text{Eq. 4})$$

$$([A] - \lambda[I])\vec{X} = 0 \quad (\text{Eq. 5})$$

$\lambda$  are the eigenvalues of the system

Using this approach no instability has been found in the speed range of interest while frequencies are closer to the experimental values than the synchronous reduced coefficients method. The predicted frequency related to the first eigenvalue is 53 Hz which is very close to the experimental instability threshold frequency (51 Hz) and it results lower than the one predicted by the use of the synchronous reduced coefficients methodology (64 Hz). The eigenvector associated with the first eigenvalue (Figure 10) shows a predominant contribution given by the top pads rotational DOFs. Second predicted eigenvalue is equal to 62 Hz and are related to bottom pads rotational DOFs (most loaded pad), this is closer in terms of frequency to those predicted by reduced synchronous coefficient method.

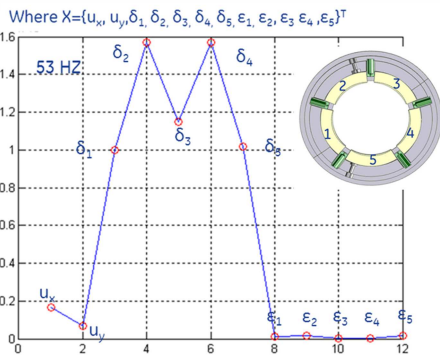


Figure 10 1<sup>st</sup> eigenvectors

(Cloud, 2010) showed by experimental activities how a full coefficients modeling of tilting pad journal bearings is capable to better predict the stability behavior of the system, at least for the base machine configuration considered.

In order to evaluate properly the natural frequencies and the related logarithmic decrements of the rotor-bearing system an explicit modeling of pad dynamics has to be used in the rotordynamic analysis, able to describe also flexibility of the shaft and especially none diagonal mass matrix including gyroscopic effect (without the hypothesis of rigid shaft previously assumed). In the rotor modeling we need to

introduce additional nodes at bearing locations to represent the 2 pad DOFs located axially ( $z$ ) at the same shaft node location (Figure 11). In this modeling, the pad inertias are lumped to the additional nodes (Dimond, 2012).

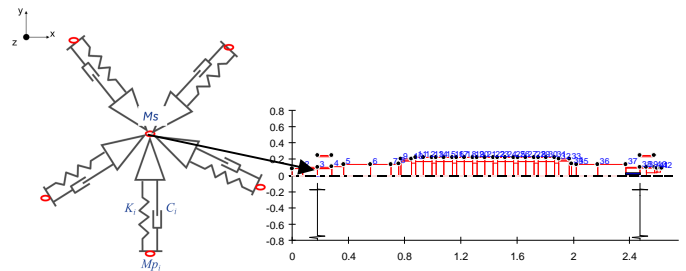


Figure 11 Explicit pads modeling

Using the Full DOFs modeling the instability onset has been calculated at 7000 rpm which is the same frequency predicted in the previous eigenvalues analysis (53 Hz). The predictions of the first eigenvalue logarithmic decrement versus speed of the two methods are compared (Figure 12).

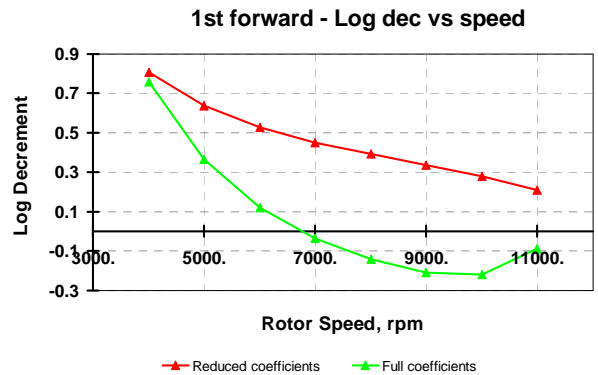


Figure 12 1<sup>st</sup> mode log. dec. vs speed

In order to validate the full DOFs methodology a new test with same bearings but a different rotor was planned.

## 2<sup>ND</sup> TEST CAMPAIGN – September 2012

### Predictions – Full DOFs approach

The second rotor (Figure 14) is representative of a rigid steam turbine rotor.

Below the most important shaft parameters:

- Bearing span: 1.579
- Total mass: 2572 Kg
- Bearing diameter: 200 mm
- Bearing length: 80 mm
- Type of load: Load on pad
- Lubrication: direct
- Test run under vacuum

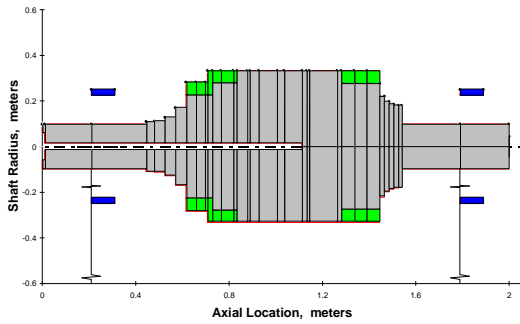


Figure 13 Rotor Scheme

The instability is predicted at 8000 rpm, 1000 rpm higher than the previous system tested. Eigenvalues calculation shows that the instability is related to top pads at 58 Hz. A number of features and parameters influencing the threshold speed were identified in pad arc length and pivot arrangement. In order to increase the stability threshold speed a new improved bearing design (Bearing B) was tested in this last rotor configuration.

The logarithmic decrement vs speed stability chart is presented (Figure 15); the red line represents the logarithmic decrement prediction using the classical reduced coefficients method (invariant for the two types of bearing), the green and the blue lines represent predictions with the full coefficients method respectively for Bearing A and Bearing B. The frequency of the 1<sup>st</sup> mode for the improved bearings configuration is predicted at 68 Hz (Figure 15).

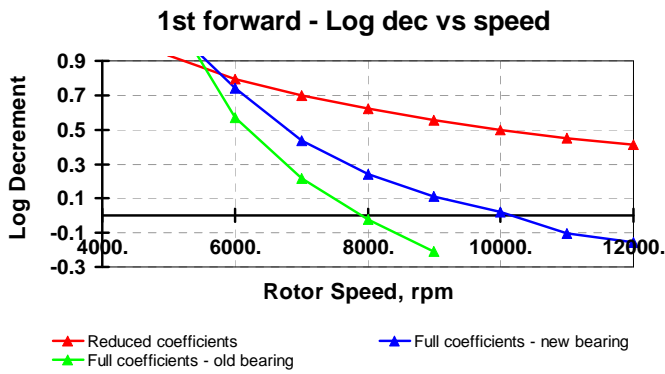


Figure 14 1<sup>st</sup> mode log. dec. vs speed

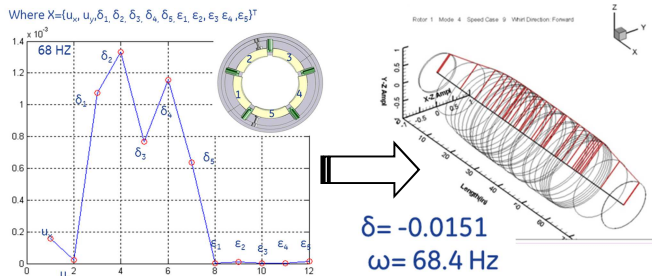


Figure 15 1<sup>st</sup> mode instability frequency

### Experimental results

During the test performed with Bearing A it was observed a subsynchronous vibration (59 Hz  $\approx$  100  $\mu$ m) appeared around 8000 rpm (Figure 16).

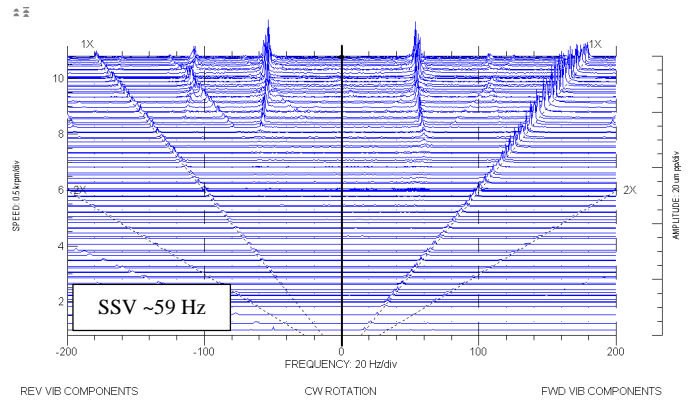


Figure 16 Cascade plot – Bearing A design - Threshold speed ~8000 rpm

The test conducted on the same rotor with the Bearing B showed a sub-synchronous incipient increase up to 9900 rpm with a frequency of 66 Hz (Figure 17).

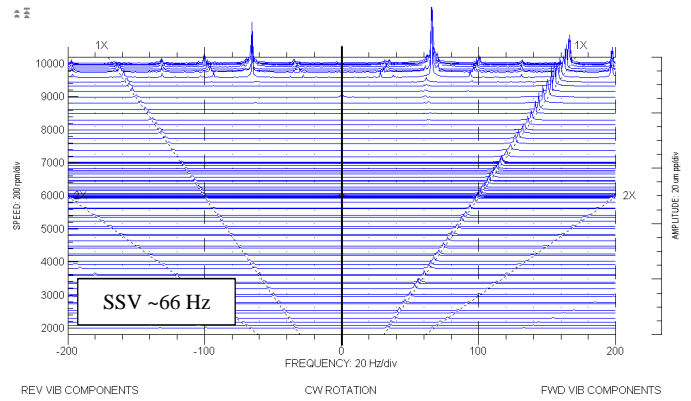
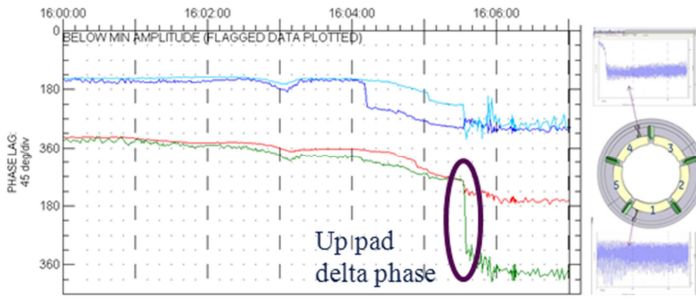


Figure 17 Cascade plot – Bearing B design - Threshold speed ~9900 rpm

Prediction for this test configuration is in good agreement with measurements. Additionally it is useful to underline that just before the rotor sub-synchronous vibration it is possible to distinguish a phase delay only for top pad while the bottom pad remained completely in phase with the rotor. The phenomena can be recognized looking at the static position change in the trend vibrations of the instrumented top pad. The static component of vibration was measured before rotor sub-synchronous vibration while no zero Hz component was measured on the bottom pad (Figure 18).



**Figure 18 Phase Bode Diagram & pad vibration in time**

The top pad main frequency component confirms the “delay of synchronization” with respect to the rotor vibration and consequently the inadequacy of the assumptions choice by the synchronous reduced method where no delay in time is possible to capture (J. Frene, 1997).

The Bearing B design has been tested also with floating end seals to understand if the changes in the boundary conditions (from an evacuated bearing to a flooded bearing) have any effect on the bearing behavior. Even if the bearing with end seals exhibits less amplitude of vibration the same sub-synchronous component appeared at the same threshold speed (Figure 1820).

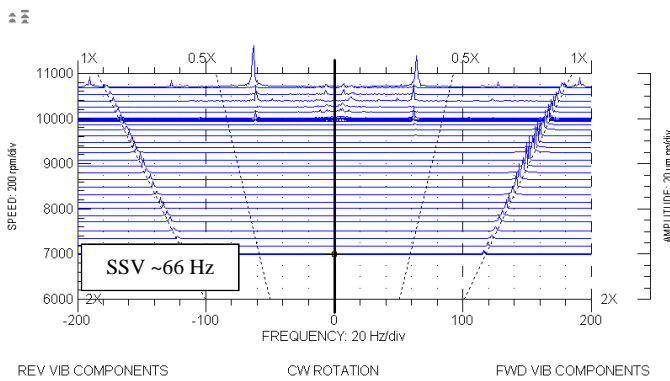


**Figure 20 Cascade plot – Bearing B design with end seals**

**Threshold speed ~9900 rpm**

## CONCLUSIONS

A test campaign has been executed to investigate the performance of an unusual combination of a large size bearings and high peripheral speed (>75 m/s).

It is very important to highlight that there is not a certain peripheral threshold speed to be considered in general a limit for a sub-synchronous issue. The same authors verified the reliability of the reduced coefficients method for the evaluation of stability threshold speed of various additional rotors equipped with smaller bearing diameters at the same peripheral speed or at different specific load.

During the test unexpected instability phenomena were observed below the target peripheral speed even if predictions using classical methods (8 reduced TPJB coefficients) predicted stable operations. A different methodology for the evaluation of instability onset has been identified to overcome the lack of predictability of the reduced coefficients method. Consequently an additional experimental activity has been conducted in order

to validate the full DOFs approach. Predicted instability threshold speeds have been observed during test with different rotors and bearings. The prediction methodology allowed identifying the main parameters influencing the onset speed position; modifications of critical features in the bearing design allowed to reach a peripheral speed of 104 m/s without any SSV. In the full DOFs method used on this job all pads are considered loaded and oil film stiffness transmits vibration from pad to the shaft (shaft+pads→coupled system), consequently no possibility of pad flutter are possible to predict. In any case pad flutter is a local instability (not transmitted to the shaft due to unloaded pad) that typically remain confined in a large sub-synchronous broad band (Decamillo, 2008) and not locked on a single frequency as the phenomena experienced during tests.

The additional experimental activities confirm the reliability of the full DOFs methodology to capture sub-synchronous incipience and allow in the future to design advanced machine architecture in terms of high speed and bearing size.

## NOMENCLATURE

$\theta_p$	= pad rotation (see figure 2)	(rad)
$\dot{\theta}_p$	= pad rotational speed	(rad/s)
$\ddot{\theta}_p$	= angular acceleration of the pad	(rad/s <sup>2</sup> )
$\xi_p$	= pad translation (see figure 2)	(m)
$\dot{\xi}_p$	= pad translation speed	(m/s)
$\ddot{\xi}_p$	= pad acceleration	(m/s <sup>2</sup> )
$\Psi$	= angle between the fixed coordinate system and the coordinate system linked to the pad	(rad)
$\omega_s$	= shaft rotating speed	(rad/s)
$C_{ii}$	= direct damping in the i direction	(Ns/m)
$C_{ik}$	= cross-coupling damping due to the i-component of force in the k direction	(Ns/m)
$[C]$	= damping matrix	(Ns/m)
$[F]$	= forces matrix	(N)
$J_p$	= pad moment of inertia	(kgm <sup>2</sup> )
$K_{ii}$	= direct stiffness in the i direction	(Ns <sup>2</sup> /m)
$K_{ik}$	= cross-coupling stiffness due to the i- component of force in the k direction	(Ns <sup>2</sup> /m)
$[K]$	= stiffness matrix	(Ns <sup>2</sup> /m)
$M_s$	= shaft mass	(kg)
$M_p$	= pad mass	(kg)
$[M]$	= mass matrix	(kg)
$u_s$	= shaft translation	(m)
$\dot{u}_s$	= shaft translation speed	(m/s)
$\ddot{u}_s$	= acceleration of the shaft	(m/s <sup>2</sup> )

APPENDIX A

<b>1<sup>ST</sup> ROTOR MATERIAL PROPERTIES</b>		
<b>Density ρ</b>	<b>Elastic Modulus E</b>	<b>Shear Modulus G</b>
<b>kg/m<sup>3</sup></b>	<b>N/m<sup>2</sup></b>	<b>N/m<sup>2</sup></b>
7850	207.0E+9	79.7E+9
<b>1<sup>ST</sup> ROTOR GEOMETRY</b>		
<b>Length</b>	<b>OD</b>	<b>ID</b>
<b>m</b>	<b>m</b>	<b>m</b>
0.073	0.160	0.000
0.106	0.160	0.000
0.100	0.160	0.000
0.087	0.222	0.000
0.189	0.268	0.000
0.149	0.268	0.000
0.052	0.263	0.000
0.015	0.280	0.000
0.075	0.347	0.000
0.030	0.309	0.000
0.058	0.338	0.000
0.058	0.338	0.000
0.030	0.309	0.000
0.058	0.338	0.000
0.058	0.338	0.000
0.030	0.309	0.000
0.058	0.338	0.000
0.058	0.338	0.000
0.030	0.309	0.000
0.058	0.338	0.000
0.058	0.340	0.000
0.030	0.311	0.000
0.058	0.340	0.000
0.058	0.338	0.000
0.030	0.309	0.000
0.058	0.338	0.000
0.058	0.338	0.000
0.030	0.309	0.000
0.058	0.338	0.000
0.058	0.338	0.000
0.030	0.309	0.000
0.075	0.347	0.000
0.015	0.280	0.000
0.038	0.260	0.000
0.149	0.268	0.000
0.201	0.268	0.067
0.100	0.184	0.067
0.043	0.184	0.080
0.063	0.184	0.139

<b>2<sup>ND</sup> ROTOR MATERIAL PROPERTIES</b>		
<b>Density ρ</b>	<b>Elastic Modulus E</b>	<b>Shear Modulus G</b>
<b>kg/m<sup>3</sup></b>	<b>N/m<sup>2</sup></b>	<b>N/m<sup>2</sup></b>
7850	207.0E+9	79.7E+9
<b>2<sup>ND</sup> ROTOR GEOMETRY</b>		
<b>Length</b>	<b>OD</b>	<b>ID</b>
<b>m</b>	<b>m</b>	<b>m</b>
0.010	0.198	0.120
0.200	0.198	0.030
0.235	0.198	0.030
0.035	0.220	0.030
0.045	0.224	0.030
0.045	0.256	0.030
0.045	0.341	0.030
0.041	0.566	0.453
0.041	0.566	0.453
0.010	0.566	0.453
0.020	0.666	0.453
0.037	0.666	0.560
0.052	0.666	0.560
0.017	0.666	0.560
0.043	0.666	0.030
0.012	0.666	0.030
0.037	0.666	0.030
0.081	0.666	0.030
0.028	0.666	0.030
0.077	0.666	0.030
0.021	0.666	0.000
0.012	0.666	0.000
0.118	0.666	0.000
0.017	0.666	0.000
0.056	0.666	0.000
0.055	0.666	0.000
0.055	0.666	0.000
0.020	0.443	0.000
0.020	0.395	0.000
0.020	0.372	0.000
0.020	0.361	0.000
0.013	0.360	0.000
0.251	0.198	0.000
0.208	0.198	0.000
0.002	0.090	0.000



## REFERENCES

- S.M. De Camillo, M. He, C. H. Cloud, J.M. Byrne, 2008, Journal Bearing vibration and SSV hash, Proceedings Of The 37th Turbomachinery Symposium.
- A. Delgado, M. Libraschi, G. Vannini, 2012, Component and System Level Testing, ASME, Turbo Expo 2012.
- T.W. Dimond, P.E. Allaire, A.A. Younan, P.N. Sheth, 2009, Tilting-pad journal bearing dynamic full coefficient and synchronous reduced proprieties using modal analysis, Proceeding of ASME Turbo Expo 2009.
- T.W. Dimond, P.E. Allaire, A.A. Youna, 2012, The Effect of Tilting Pad Journal Bearing Dynamic Models on the Linear Stability Analysis of an 8-Stage Compressor, Journal of Engineering For Gas Turbines ASME 2012.
- J. Frene and D. Nicolas, 1997, *Hydrodynamic lubrication*, Elsevier.
- C. H. Cloud, E.H. Maslen, L.E. Barrett, 2010, Influence of tilting pad journal bearing model on rotor stability estimation, 8th IFToMM International Conference On Rotordynamic.
- J.W. Lund, 1964, Spring and damping coefficients for the Tilting-pad journal bearing, ASLE Transaction Volume 7.
- W.Shapiro, A. Colsher, 1977, Dynamic characteristic of fluid-film bearings, Proceedings of the 6th Turbomachinery Symposium, Texas A&M University.

## ACKNOWLEDGEMENTS

The authors thank GE Oil&Gas for allowing the publication of this work. Particular thanks to our colleagues Adolfo Delgado that helped and supported us with him authoritative expertise during all the tests.